# Appendix A

# Calculation of Human Equivalent Continuous Exposure Concentrations (HECs)

## 1 A.1. INTRODUCTION

As discussed in Chapter 3, the lung burden of diesel particulate matter (DPM) during exposure is determined by both the amount and site of particle deposition in the lung and, subsequently, by rates of translocation and clearance from the deposition sites. Mathematical models have often been used to complement experimental studies in estimating the lung burdens of inhaled particles in different species under different exposure conditions. This appendix presents a mathematical model that simulates the deposition and clearance of DPM in the lungs of rats and humans of Yu et al.(1991) also published as Yu and Yoon (1990).

9 Diesel particles are aggregates formed from primary spheres 15-30 nm in diameter. The 10 aggregates are irregularly shaped and range in size from a few molecular diameters to tens of 11 microns. The mass median aerodynamic diameter (MMAD) of the aggregates is typically 0.2 µm 12 and is polydisperse with a geometric standard deviation of around 2.3. The organics adsorbed 13 onto the aggregates normally account for 10% to 30% of the particle mass. However, the exact 14 size distribution of DPM and the specific composition of the adsorbed organics depend upon 15 many factors, including engine design, fuels used, engine operating conditions, and the thermodynamic process of exhaust. The physical and chemical characteristics of DPM have been 16 17 reviewed extensively by Amann and Siegla (1982) and Schuetzle (1983).

Four mechanisms deposit DPM within the respiratory tract during exposure: impaction, sedimentation, interception, and diffusion. The contribution from each mechanism to deposition, however, depends upon lung structure and size, the breathing condition of the subject, and particle size distribution. Under normal breathing conditions, diffusion is the most dominant mechanism and the other three mechanisms play minor roles.

Once DPM is deposited in the respiratory tract, both the carbonaceous core and the adsorbed organics will be removed from the deposition sites by mechanical clearance, provided by mucociliary transport in the ciliated conducting airways as well as macrophage phagocytosis and migration in the nonciliated airways, and dissolution. As the carbonaceous core or soot of DPM is insoluble, it is removed from the lung primarily by mechanical clearance, whereas the adsorbed organics are removed principally by dissolution (Chapter 3).

29 30

## A.2. PARTICLE MODEL

To develop a mathematical model that simulates the deposition and clearance of DPM in the lung, an appropriate model for diesel particles must be introduced. For the deposition study, an equivalent sphere model developed by Yu and Xu (1987) was used to simulate the dynamics and deposition of DPM in the respiratory tract by various mechanisms. For the clearance study, a diesel particle is assumed to be composed of three different material components according to

1 their characteristic clearance rates: (1) a carbonaceous core of approximately 80% of the particle 2 mass; (2) absorbed organics of about 10% of particle mass, which are slowly cleared from the 3 lung; and (3) adsorbed organics quickly cleared from the lung, accounting for the remaining 10% 4 of particle mass. The presence of two discrete organic phases in the particle model is suggested by observations that the removal of particle-associated organics from the lung exhibits a biphasic 5 6 clearance curve (Sun et al., 1984; Bond et al., 1986), as discussed in Chapter 3. This curve 7 represents two major kinetic clearance phenomena: a fast- phase organic washout with a half-8 time of a few hours, and a slow phase with a half-time that is a few hundred times longer. The 9 detailed components involved in each phase are not known. It is possible that the fast phase 10 consists of organics that are leached out primarily by diffusion mechanisms while the slow phase might include any or all of the following components: (a) organics that are "loosened" before 11 12 they are released, (b) organics that have become intercalated in the carbon core and whose release 13 is thus impeded, (c) organics that are associated for longer periods of time because of 14 hydrophobic interaction with other organic-phase materials, (d) organics that have been ingested 15 by macrophages and as a result effectively remain in the lung for a longer period of time because 16 of metabolism by the macrophage (metabolites formed may interact with other cellular 17 components), and (e) organics that have directly acted on cellular components, such as the 18 formation of covalent bonds with DNA and other biological macromolecules to form adducts.

19 The above distinction of the organic components is general and made to account for the 20 biphasic clearance of DPM; it does not specifically imply the actual nature of the adsorbed 21 organics. For aerosols made of pure organics, such as benzo(a)pyrene (BaP) and nitropyrene 22 (NP) in the same size range of DPM, Sun et al. (1984) and Bond et al. (1986) observed a nearly 23 monophasic clearance curve. This might be explained by the absence of intercalative phenomena 24 (a) and of hydrophobic interaction imposed by a heterogeneous mixture of organics (b). The 25 measurement of a pure organic might also neglect that quantity which has become intracellularly 26 (c) or covalently bound (d).

27

28

## A.3. COMPARTMENTAL LUNG MODEL

The model of Yu et al. (1991) comprises three principal compartments involved in deposition and clearance: tracheobronchial (T or TB), alveolar (A), and lung-associated lymph node (L), as shown in Figure A-1. The outside compartments blood (B) and GI tract (G) and nasopharyngeal or head (H) are also represented. The alveolar compartment in the model is obviously the most important for long-term retention studies. However, for short-term consideration, retentions in other lung compartments may also be significant. The presence of

- 1 these lung compartments and the two outside compartments in the model therefore provides a
- 2 complete description of all clearance processes involved.
- In Figure A-1,  $r_{H^{*}}^{(i)}$   $r_{T^{*}}^{(i)}$  and  $r_{A}^{(i)}$  are, respectively, the mass deposition rates of DE material component i (i=1 [core], 2 [slowly cleared organics], and 3 [rapidly cleared organics]) in the head, tracheobronchial, and alveolar compartments; and  $\lambda_{XY}^{(i)}$  represents the transport rate of material component i from any compartment X to any compartment Y. Let the mass fraction of material component i of a diesel particle be  $f_i$ . Then

$$r_{H}^{(i)} = f_{i} r_{H} ,$$
 (A-1)

$$r_T^{(i)} = f_i r_T , \qquad (A-2)$$

$$r_A^{(i)} = f_i r_A , \qquad (A-3)$$

- 9 where  $r_{H}$ ,  $r_{T}$ , and  $r_{A}$  are, respectively, the total mass deposition rates of DPM in the H, T, and 10 A compartments, determined from the equations: 11 12 13  $r_{H} = c(TV)(RF)(DF)_{H}$ , (A-4)
- 14

$$r_T = c(TV)(RF)(DF)_T , \qquad (A-5)$$

15

$$r_A = c(TV)(RF)(DF)_A \quad . \tag{A-6}$$

16

17

1 In Equations A-4 to A-6, c is the mass concentration of DPM in the air, TV is the tidal 2 volume, RF is the respiratory frequency, and  $(DF)_{H}$ ,  $(DF)_{T}$ , and  $(DF)_{A}$  are, respectively, the 3 deposition fractions of DPM in the H, T, and A compartments over a respiratory cycle. The 4 values of  $(DF)_{H}$ ,  $(DF)_{T}$ , and  $(DF)_{A}$ , which vary with the particle size, breathing conditions, and 5 lung architecture, were determined from the deposition model of Yu and Xu (1987).

6 The differential equations for m<sup>(i)</sup><sub>XY</sub>, the mass of material component i in compartment X as a
7 function of exposure time t, can be written as

- 8
- 9 Head (H)

$$\frac{dm_{H}^{(i)}}{dt} = r_{H}^{(i)} - \lambda_{HG}^{(i)}m_{H}^{(i)} - \lambda_{HB}^{(i)}m_{H}^{(i)} , \qquad (A-7)$$

$$\frac{dm_T^{(i)}}{dt} = r_T^{(i)} + \lambda_{AT}^{(i)} m_A^{(i)} - \lambda_{TG}^{(i)} m_T^{(i)} - \lambda_{TB}^{(i)} m_T^{(i)} , \qquad (A-8)$$

11 Alveolar (A)

12

$$\frac{dm_A^{(i)}}{dt} = r_A^{(i)} - \lambda_{AT}^{(i)} m_A^{(i)} - \lambda_{AL}^{(i)} m_A^{(i)} - \lambda_{AB}^{(i)} m_A^{(i)} , \qquad (A-9)$$

#### 13 Lymph nodes (L)

$$\frac{dm_L^{(i)}}{dt} = \lambda_{AL}^{(i)} m_A^{(i)} - \lambda_{LB}^{(i)} m_L^{(i)} .$$
 (A-10)

#### 14 Equation A-9 may also be written as

$$\frac{dm_A^{(i)}}{dt} = r_A^{(i)} - \lambda_A^{(i)} m_A^{(i)} , \qquad (A-11)$$

$$\lambda_{A}^{(i)} = \lambda_{AT}^{(i)} + \lambda_{AL}^{(i)} + \lambda_{AB}^{(i)} .$$
 (A-12)

is the total clearance rate of material component i from the alveolar compartment. In Equations
 A-7 to A-10, we have assumed vanishing material concentration in the blood compartment to
 calculate diffusion transport.

The total mass of the particle-associated organics in compartment X is the sum of  $m_X^{(2)}$  and  $m_X^{(3)}$  the total mass of DPM in compartment X is equal to

3

$$m_X = m_X^{(1)} + m_X^{(2)} + m_X^{(3)}$$
 (A-13)

5 The lung burdens of diesel soot (core) and organics are defined, respectively, as

6

4

$$m_{Lung}^{(1)} = m_T^{(1)} + m_A^{(1)}$$
, (A-14)

7

8 and

9

 $m_{Lung}^{(2)+(3)} = m_T^{(2)} + m_A^{(2)} + m_T^{(3)} + m_A^{(3)}$  (A-15)

10

11Because the clearance of diesel soot from compartment T is much faster than from compartment12A,  $m_T^{(I)} < m_A^{(I)}$  a short time after exposure, Equation A-14 leads to

13

 $m_{Lung}^{(1)} \cong m_A^{(1)}$  (A-16)

14

Solution to Equations A-7 to A-10 can be obtained once all the transport rates  $\lambda_{XY}^{(i)}$  are 15 known. When  $\lambda_{XY}^{(i)}$  are constant, which is the case in linear kinetics, Equations A-7 to A-10 will 16 17 have a solution that increases with time at the beginning of exposure but eventually saturates and 18 reaches a steady-state value. This is the classical retention model developed by the International 19 Commission of Radiological Protection (ICRP, 1979). However, as discussed in Chapter 3, data 20 have shown that when rats are exposed to DPM at high concentration for a prolonged period, 21 long-termed clearance is impaired. This is the so-called overload effect, observed also for other 22 insoluble particles. The overload effect cannot be predicted by the classical ICRP model. 23 Soderholm (1981) and Strom et al. (1987, 1988) have proposed a model to simulate this effect by 24 adding a separate sequestering compartment in the alveolar region. In the present approach, a 25 single compartment for the alveolar region of the lung is used and the overload effect is accounted for by a set of variable transport rates  $\lambda_{AD}^{(i)}$ ,  $\lambda_{AL}^{(i)}$ , and  $\lambda_{A}^{(i)}$  which are functions of  $m_A$ . The transport 26

- 1 rates  $\lambda_A^{(i)}$  and  $\lambda_{AL}^{(i)}$  in Equations A-7 to A-10 can be determined directly from experimental data on 2 lung and lymph node burdens, and  $\lambda_{AT}^{(i)}$  and  $\lambda_{AB}^{(i)}$  from Equation A-12.
- 3

## A.4. SOLUTIONS TO KINETIC EQUATIONS

Equation A-11 is a nonlinear differential equation of m<sub>A</sub><sup>(i)</sup> with known function of λ<sub>A</sub><sup>(i)</sup>.
 For diesel soot, this equation becomes

7

$$\frac{dm_A^{(1)}}{dt} = r_A^{(1)} - \lambda_A^{(1)}(m_A)m_A^{(1)} .$$
 (A-17)

8

9 Because clearance of the particle-associated organics is much faster than diesel soot,  $m_A^{(2)}$  and  $m_A^{(3)}$ 

10 constitute only a very small fraction of the total particle mass (less than 1%) after a long

11 exposure, and we may consider  $\lambda_A^{(1)}$  as a function of  $m_A^{(1)}$  alone. Equation A-17 is then reduced to a

12 differential equation with  $m_A^{(1)}$  the only dependent variable.

13 The general solution to Equation A-17 for constant  $r_A^{(1)}$  at any time, t, can be obtained by 14 the separation of variables to give

15

$$\int_{0}^{m_{A}^{(1)}} \frac{dm_{A}^{(1)}}{r_{A}^{(1)} - \lambda_{A}^{(1)} m_{A}^{(1)}} = t .$$
 (A-18)

16

17 If  $r_A^{(1)}$  is an arbitrary function of t, Equation A-17 needs to be solved numerically such as by 18 a Runge-Kutta method. Once  $m_A^{(1)}$  is found, the other kinetic equations A-7 to A-10 for both diesel 19 soot and the particle-associated organics can be solved readily, as they are linear equations. The 20 solutions to these equations for constant  $r_H^{(i)}$ ,  $r_T^{(i)}$ , and  $r_A^{(i)}$  are given below: 21 Head (H)

22

$$m_{H}^{(i)} = r_{H}^{(i)} / \lambda_{H}^{(i)} + (m_{H0}^{(i)} - r_{H}^{(i)}) / \lambda_{H}^{(i)}) \exp(-\lambda_{H}^{(i)} t)$$
(A-19)

23

where 
$$\lambda_{H}^{(i)} = \lambda_{HG}^{(i)} + \lambda_{HB}^{(i)}$$
 (A-20)

24

A-7 DRAFT—DO NOT CITE OR QUOTE

#### 2 Tracheobronchial (T)

3

$$m_T^{(i)} = \exp(-\lambda_T^{(i)} t) \int_0^t (r_T^{(i)} + \lambda_{AT}^{(i)} m_A^{(i)}) \exp(\lambda_T^{(i)} t) dt + m_{T0}^{(i)}$$
(A-21)

where 
$$\lambda_T^{(i)} = \lambda_{TG}^{(i)} + \lambda_{TB}^{(i)}$$
 (A-22)

4

5 Lymph nodes (L)

6

$$m_L^{(i)} = \exp(-\lambda_{LB}^{(i)} t) \int_0^t \lambda_{AL}^{(i)} m_A^{(i)} \exp(\lambda_{LB}^{(i)} t) dt + m_{L0}^{(i)})$$
(A-23)

7

8 In Equations A-19 to A-23,  $m_{XO}^{(i)}$  represents the value of  $m_X^{(i)}$  at t = 0. 9 In the sections to follow, the methods of determining  $r_{H}^{(i)}$ ,  $r_T^{(i)}$  and  $r_A^{(i)}$ , or (DF)<sub>H</sub>, (DF)<sub>T</sub>, and 10 (DF)<sub>A</sub>  $r_{H}^{(DF)}$ ,  $r_{T}^{(DF)}$ , and  $r_{A}^{(DF)}$  as well as the values of  $\lambda_{XY}^{(i)}$  in the compartmental lung model are 11 presented.

**A.5. DETERMINATION OF DEPOSITION FRACTIONS** 

12

#### 13

14 The mathematical models for determining the deposition fractions of DPM in various 15 regions of the respiratory tract have been developed by Yu and Xu (1986, 1987) and are adopted 16 in this report. Yu and Xu consider DPM as a polydisperse aerosol with a specified mass median 17 aerodynamic diameter (MMAD) and geometrical standard deviation  $\sigma_{g}$ . Each diesel particle is 18 represented by a cluster-shaped aggregate within a spherical envelope of diameter  $d_{e}$ . The 19 envelope diameter  $d_{e}$  is related to the aerodynamic diameter of the particle by the relation 20

$$\frac{d_e}{d_a} = \phi^{-1/2} (\frac{C_a}{C_e})^{1/2} (\frac{\zeta}{\zeta_o})^{1/2}$$
(A-24)

21

1 where  $\zeta$  is the bulk density of the particle in g/cm<sup>3</sup>,  $\zeta_0 = 1$  g/cm<sup>3</sup>;  $\varphi$  is the packing density, which 2 is the ratio of the space actually occupied by primary particles in the envelope to the overall

3 envelope volume; and  $C_x$  is the slip factor given by the expression:

4

$$C_x = 1 + 2\frac{\lambda}{d_x} \left[1.257 + 0.4 \exp \left[-\left(\frac{0.55d_x}{\lambda}\right)\right]\right]$$
 (A-25)

5

in which λ ≈ 8 × 10<sup>-6</sup>cm<sup>3</sup> is the mean free path of air molecules at standard conditions. In the
diesel particle model of Yu and Xu (1986), ζ has a value of 1.5 g/cm<sup>3</sup> and a φ value of 0.3 is
chosen based upon the best experimental estimates. As a result, Equation A-24 gives d<sub>e</sub>/d<sub>a</sub> = 1.35.
In determining the deposition fraction of DPM, d<sub>e</sub> is used for diffusion and interception according
to the particle model.

11

12 A.5.1. Deposition in the Head

13 Particle deposition in the naso- or oropharyngeal region is referred to as head or extrathoracic deposition. The amount of particles that enters the lung depends upon the breathing 14 mode. Normally, more particles are collected via the nasal route than by the oral route because of 15 the nasal hairs and the more complex air passages of the nose. Since the residence time of diesel 16 17 particles in the head region during inhalation is very small (about 0.1 s for human adults at normal 18 breathing), diffusional deposition is insignificant and the major deposition mechanism is impaction. 19 The following empirical formulas derived by Yu et al. (1981) for human adults are adopted for 20 deposition prediction of DPM:

For mouth breathing:

$$(DF)_{H, in} = 0, \text{ for } d_a^2 \le 3000$$
 (A-26)

22

$$(DF)_{H, in} = -1.117 + 0.324 \log(d_a^2 Q), \text{ for } d_a^2 Q > 3000$$
 (A-27)

$$(DF)_{H, ex} = 0,$$
 (A-28)

23

- and for nose breathing:
- 25

$$(DF)_{H, in} = -0.014 + 0.023 \log(d_a^2 Q), \text{ for } d_a^2 Q \le 337$$
 (A-29)

7/25/00

A-9 DRAFT—DO NOT CITE OR QUOTE

$$(DF)_{H, ex} = -0.851 + 0.399 \log(d_a^2 Q), \text{ for } d_a^2 Q > 215$$
 (A-32)

$$(DF)_{H, in} = -0.959 + 0.397 \log(d_a^2 Q), \text{ for } d_a^2 Q > 337$$
 (A-30)

$$(DF)_{H, ex} = 0.003 + 0.033 \log(d_a^2 Q), \text{ for } d_a^2 Q \le 215$$
 (A-31)

where (DF)<sub>H</sub> is the deposition efficiency in the head, the subscripts in and ex denote inspiration
and expiration, respectively, d<sub>a</sub> is the particle aerodynamic diameter in µm, and Q is the air
flowrate in cm<sup>3</sup>/sec.

Formulas to calculate deposition of diesel particles in the head region of children are
derived from those for adults using the theory of similarity, which assumes that the air passage in
the head region is geometrically similar for all ages and that the deposition process is
characterized by the Stokes number of the particle. Thus, the set of empirical equations from
A-26 through A-32 are transformed into the following form:
For mouth breathing:

$$(DF)_{H, in} = 0, \text{ for } d_a^2 Q \le 3000$$
 (A-33)

13 and for nose breathing:

$$(DF)_{H, in} = -1.117 + 0.972 \log K + 0.324 \log(d_a^2 Q), \text{ for } d_a^2 Q > 3000$$
 (A-34)

$$(DF)_{H, ex} = 0.$$
 (A-35)

$$(DF)_{H, in} = -0.014 + 0.690 \log K + 0.023 \log(d_a^2 Q), \text{ for } d_a^2 Q \le 337$$
 (A-36)

$$(DF)_{H, in} = -0.959 + 1.191 \log K + 0.397 \log (d_a^2 Q), \text{ for } d_a^2 Q > 337$$
 (A-37)

7/25/00

A-10 DRAFT—DO NOT CITE OR QUOTE

$$(DF)_{H, ex} = 0.003 + 0.099 \log K + 0.033 \log(d_a^2 Q), \text{ for } d_a^2 Q \le 215$$
 (A-38)

$$(DF)_{H, ex} = 0.851 + 1.197 \log K + 0.399 \log(d_a^2 Q), \text{ for } d_a^2 Q > 215$$
 (A-39)

where K is the ratio of the linear dimension of the air passages in the head region of adults to that
of children, which is assumed to be the same as the ratio of adult/child tracheal diameters.

4 For rats, the following empirical equations are used for deposition prediction of DPM in5 the nose:

$$(DF)_{H, in} = (DF)_{H, ex} = 0.046 + 0.009 \log(d_a^2 Q), \text{ for } d_a^2 Q \le 13.33$$
 (A-40)

## 6 7

#### A.5.2. Deposition in the Tracheobronchial and Alveolar Regions

8 The deposition model adopted for DPM is the one previously developed for monodisperse
9 (Yu, 1978) and polydisperse spherical aerosols (Diu and Yu, 1983). In the model,

$$(DF)_{H, in} = (DF)_{H, ex} = -0.522 + 0.514 \log(d_a^2 Q), \text{ for } d_a^2 Q > 13.33$$
 (A-41)

10

the branching airways are viewed as a chamber model shaped like a trumpet (Figure A-2). The cross-sectional area of the chamber varies with airway depth, x, measured from the beginning of the trachea. At the last portion of the trumpet, additional cross-sectional area is present to account for the alveolar volume per unit length of the airways. Inhaled diesel particles that escape capture in the head during inspiration will enter the trachea and subsequently the bronchial airways (compartment T) and alveolar spaces (compartment A).

Assuming that the airways expand and contract uniformly during breathing, the equationfor the conservation of particles takes the form:

19

$$\beta(A_1 + A_2)\frac{\partial c}{\partial x} + Q \frac{\partial c}{\partial x} = -Qc\eta \qquad (A-42)$$

20

where c is the mean particle concentration at a given x and time t;  $A_1$  and  $A_2$  are, respectively, the summed cross-sectional area (or volume per unit length) of the airways and alveoli at rest;  $\eta$  is the particle uptake efficiency per unit length of the airway;  $\beta$  is an expansion factor, given by:

$$\beta = 1 + \frac{V_t}{V_l} \tag{A-43}$$

2 and Q is the air flow rate, varying with x and t according to the relation

$$\frac{Q}{Q_o} = 1 - \frac{V_x}{V_l} \tag{A-44}$$

3

1

4 where  $Q_0$  is the air flow rate at x = 0. In Equations A-43 and A-44, V<sub>t</sub> is the volume of new air in 5 the lungs and V<sub>x</sub> and V<sub>e</sub> are, respectively, the accumulated airway volume from x = 0 to x, and 6 total airway volume at rest.

Figure 1
Equation A-42 is solved using the method of characteristics with appropriate initial and
boundary conditions. The amount of particles deposited between location x<sub>1</sub> and x<sub>2</sub> from time t<sub>1</sub>
to t<sub>2</sub> can then be found from the expression

10

$$DF = \int_{t_1}^{t_2} \int_{x_1}^{x_2} Qc \eta dx dt$$
 (A-45)

11

For diesel particles, η is the sum of those due to the individual deposition mechanisms
described above, i.e.,

14 where  $\eta_I$ ,  $\eta_S$ ,  $\eta_P$ , and  $\eta_D$  are, respectively, the deposition efficiencies per unit length of the airway

 $\eta = \eta_I + \eta_S + \eta_P + \eta_D \tag{A-46}$ 

15 due to impaction, sedimentation, interception, and diffusion. On the basis of the particle model 16 described above, the expressions for  $\eta_I$ ,  $\eta_S$ ,  $\eta_P$ , and  $\eta_D$  are obtained in the following form: 17

$$\eta_I = \frac{0.768}{L} (St)\theta. \tag{A-47}$$

18

19 
$$\eta_{s} = \frac{2}{\pi L} [2\epsilon \sqrt{1 - \epsilon^{(2/3)}} - \epsilon^{1/3} \sqrt{1 - \epsilon^{2/3}} + \sin^{-1} \epsilon^{1/3}]$$
(A-48)

A-12 DRAFT—DO NOT CITE OR QUOTE

$$\eta_P = \frac{4}{3\pi L} (\Gamma - \frac{\Gamma^3}{32})$$
 (A-49)

$$\eta_D = \frac{1}{L} [1 - 0.819 \exp(-14.63\Delta) - 0.0976 \exp(-89.22\Delta) - (A-50)$$

$$0.0325 \exp(-228\Delta) - 0.0509 \exp(-125\Delta^{2/3})]$$

$$0.0323 \exp(-228\Delta) = 0.030$$

$$\eta_D = \frac{4}{L} \Delta^{1/2} \ (1 \ - \ 0.444 \Delta^{1/2}) \tag{A-51}$$

2

for Reynolds numbers of the flow smaller than 2000, and for Reynolds numbers greater than or equal to 2000, where  $ST = d_a^2 u/(18\mu R)$  is the particle Stokes number,  $\theta = L/(8R)$ ,  $\epsilon =$  $3\mu u_s L/(32uR)$ ,  $\Gamma = d_e/R$ , and  $\Delta = DL/(4R^2u)$ . In the above definitions u is the air velocity in the airway;  $\mu$  is the air viscosity; L and R are, respectively, the length and radius of the airway;  $u_s =$  $C_a d_a^2/(18\mu)$  is the particle settling velocity; and  $D = C_e kT(3\pi\mu d_e)$  is the diffusion coefficient with k denoting the Boltzmann constant and T the absolute temperature. In the deposition model, it is also assumed that  $\eta_I$  and  $\eta_P = 0$  for expiration, while  $\eta_D$  and  $\eta_S$  have the same expressions for

10 both inspiration and expiration.

During the pause, only diffusion and sedimentation are present. The combined deposition
efficiency in the airway, E, is equal to:

13

$$E = 1 - (1 - E_S) (1 - E_D) .$$
 (A-52)

14

where  $E_D$  and  $E_S$  are, respectively, the deposition efficiencies due to the individual mechanisms of diffusion and sedimentation over the pause period. The expression for  $E_D$  and  $E_S$  are given by

$$E_{D} = 1 - \sum_{i=1}^{3} \frac{4}{\alpha_{i}} \exp(-\alpha_{i}^{2}\tau_{D})(1 - \sum_{i=1}^{3} \frac{4}{\alpha_{i}^{2}}) \exp\left[-\frac{4\tau_{D}^{1/2}}{\pi^{1/2}(1 - \sum_{i=1}^{3} \frac{4}{\alpha_{i}^{2}})}\right]$$
(A-53)

18

A-13 DRAFT—DO NOT CITE OR QUOTE

1 where  $\tau_{\rm D} = D\tau/R^2$  in which  $\tau$  is the pause time and  $\alpha_1$ ,  $\alpha_2$ , and  $\alpha_3$  are the first three roots of the

2 equation:

$$J_{\rho}(\alpha) = 0 . \qquad (A-54)$$

## 3 in which $J_o$ is the Bessel function of the zero<sub>th</sub> order, and:

4

$$E_{s} = 1.1094\tau_{s} - 0.1604\tau_{s}^{2}, \text{ for } 0 < \tau_{s} \le 1.$$
 (A-55)

5

6 and

$$E_{s} = 1 - 0.0069\tau_{s}^{-1} - 0.0859\tau_{s}^{-2} - 0.0582\tau_{s}^{-3},$$
  
for  $\tau_{s} > 1,$  (A-56)

7 where  $\tau_{\rm S} = u_{\rm S} \tau / 2 R$ .

8 The values of (DF)<sub>T</sub> and (DF)<sub>A</sub> over a breathing cycle are calculated by superimposing
9 DF for inspiration, deposition efficiency E during pause, and DF for expiration in the
10 tracheobronchial airways and alveolar space. It is assumed that the breathing cycle consists of a
11 constant flow inspiration, a pause, and a constant flow expiration, each with a respective duration
12 fraction of 0.435, 0.05, and 0.515 of a breathing period.

13

## 14 A.5.3. Lung Models

Lung architecture affects particle deposition in several ways: the linear dimension of the airway is related to the distance the particle travels before it contacts the airway surface; the air flow velocity by which the particles are transported is determined by the cross-section of the airway for a given volumetric flowrate; and flow characteristics in the airways are influenced by the airway diameter and branching patterns. Thus, theoretical prediction of particle deposition depends, to a large extent, on the lung model chosen.

21

## 22 A.5.3.1. Lung Model for Rats

Morphometric data on the lung airways of rats were reported by Schum and Yeh (1979). Table A-1 shows the lung model data for Long Evans rats with a total lung capacity of 13.784 cm<sup>3</sup>. Application of this model to Fischer rats is accomplished by assuming that the rat has the same lung structure regardless of its strain and that the total lung capacity is proportional to the body weight. In addition, it is also assumed that the lung volume at rest is about 40% of the total lung capacity and that any linear dimension of the lung is proportional to the cubic rootof the lung volume.

3

## 4 A.5.3.2. Lung Model for Human Adults

5 The lung model of mature human adults used in the deposition calculation of DPM is the 6 symmetric lung model developed by Weibel (1963). In Weibel's model, the airways are assumed 7 to be a dichotomous branching system with 24 generations. Beginning with the 18th generation, 8 increasing numbers of alveoli are present on the wall of the airways, and the last three generations 9 are completely aleveolated. Thus, the alveolar region in this model consists of all the airways in 10 the last seven generations. Table A-2 presents the morphometric data of the airways of Weibel's 11 model adjusted to a total lung volume of 3000 cm<sup>3</sup>.

12

### 13 A.5.3.3. Lung Model for Children

The lung model for children in the diesel study was developed by Yu and Xu (1987) on the basis of available morphometric measurements. The model assumes a lung structure with dichotomous branching of airways, and it matches Weibel's model for a subject when evaluated at the age of 25 years, the age at which the lung is considered to be mature. The number and size of airways as functions of age t (years) are determined by the following equations.

A.5.3.3.1. *Number of airways and alveoli*. The number of airways N<sub>i</sub>(t) at generation i for age t
 is given by

$$N_i(t) = 2^i,$$
 for  $0 \le i \le 20$  (A-57)

22

19

$$\begin{cases} N_{21}(t) = N_r(t), \\ N_{22}(t) = N_{23}(t) = 0. \end{cases} \text{ for } N_r(t) \le 2^{21} \tag{A-58}$$

23

24

$$\begin{cases} N_{21}(t) = 2^{21}, \\ N_{22}(t) = N_r(t) - 2^{21}, \\ N_{23}(t) = 0, \end{cases} \text{ for } 2^{21} < N_r(t) \le 2^{22} \qquad (A-59)$$

25

$$N_{21}(t) = 2^{21},$$
  

$$N_{22}(t) = 2^{22},$$
  

$$N_{23}(t) = N_r(t) - 2^{21} - 2^{22}$$
  
for  $N_r(t) > 2^{21} + 2^{22},$   
(A-60)

1 where  $N_r(t)$  is the total number of airways in the last three airway generations. The empirical 2 equation for  $N_r$  which best fits the available data is

3

4 Thus,  $N_r(t)$  increases from approximately 1.5 million at birth to 15 million at 8 years of age and

$$N_r(t) = \begin{cases} 2.036 \times 10^7 (1 - 0.926e^{-0.15}t), & t \le 8\\ 1.468 \times 10^7, & t > 8 \end{cases}$$
(A-61)

remains nearly constant thereafter. Equations A-58 to A-60 also imply that in the last three
generations, the airways in the subsequent generation begin to appear only when those in the
preceding generation have completed development.

8 The number of alveoli as a function of age can be represented by the following equation9 according to the observed data:

10

$$N_A(t) = 2.985 \times 10^8 (1 - 0.919e^{-0.45}t)$$
 (A-62)

11

The number of alveoli distributed in the unciliated airways at the airway generation level is determined by assuming that alveolization of airways takes place sequentially in a proximal direction. For each generation, alveolization is considered to be complete when the number of alveoli in that generation reaches the number determined by Weibel's model.

16

A.5.3.3.2. Airway size. Four sets of data are used to determine airway size during postnatal
growth: (a) total lung volume as a function of age; (b) airway size as given by Weibel's model;
(c) the growth pattern of the bronchial airways; and (d) variation in alveolar size with age. From
these data, it is found that the lung volume, LV(t) at age t, normalized to Weibel's model at 4800
cm<sup>3</sup> for an adult (25 years old), follows the equation

22

$$LV(t) = 0.959 \times 10^5 (1 - 0.998e^{-0.002}t) (cm^3).$$
 (A-63)

23 24

25

7/25/00

The growth patterns of the bronchial airways are determined by the following equations

$$D_i(t) - D_{iw} = \alpha_i [H(t) - H(25)],$$
 (A-64)

$$L_i(t) - L_{iw} = \beta_i [H(t) - H(25)],$$
 (A-65)

where D<sub>i</sub>(t) and L<sub>i</sub>(t) are, respectively, the airway diameter and length at generation i and age t,
 D<sub>iw</sub> and L<sub>iw</sub> the corresponding values for Weibel's model, α<sub>i</sub> and β<sub>i</sub> are coefficients given by

$$\alpha_i = 3.26 \times 10^{-2} \exp[-1.183 \ (i+1)^{0.5}]$$
 (A-66)

$$\beta_i = 1.05 \times 10^{-6} \exp [10.1] (i+1)^{-0.2}$$
 (A-67)

6 and H(t) is the body height, which varies with age t in the form

$$H(t) = 1.82 \times 10^{2} (1 - 0.725e^{-0.14}t) \ (cm). \tag{A-68}$$

$$\frac{D_i}{D_{iw}} = \frac{L_i}{L_{iw}} = \frac{D_a}{D_{aw}} = f(t), \quad for \ 17 \le i \le 23$$
(A-69)

12 where  $D_a$  is the diameter of an alveolus at age t,  $D_{aw} = 0.0288$  cm is the alveolar diameter for 13 adults in accordance with Weibel's model, and f(t) is a function determined from 

$$f(t) = \sqrt[3]{\frac{\{LV(t) - \sum_{i=0}^{16} \frac{\pi}{4} D_i^2(t) \ L_i(t) N_i(t)\}}{\{\sum_{i=17}^{23} \frac{\pi}{4} D_{iw}^2 L_{iw} N_i(t) + \frac{5\pi}{36} D_{aw}^3 N_A(t)\}}}$$
(A-70)

## 1 A.6. TRANSPORT RATES

The values of transport rates  $\lambda_{XY}^{(i)}$  for rats have been derived from the experimental data of clearance for diesel soot (Chan et al., 1981; Strom et al., 1987, 1988) and for the particleassociated organics (Sun et al., 1984; Bond et al., 1986; Yu et al., 1991). These values are used in the present model of lung burden calculation and are listed below:

$$\lambda_{HG}^{(i)} = 1.73 \ (i = 1, 2, 3) \tag{A-71}$$

6

$$\lambda_{HB}^{(1)} = \lambda_{TB}^{(1)} = \lambda_{LB}^{(1)} = \lambda_{AB}^{(i)} = 0.00018$$
 (A-72)

7

$$\lambda_{HB}^{(2)} = \lambda_{TB}^{(2)} = \lambda_{LB}^{(2)} = \lambda_{AB}^{(2)} = 0.0129$$
 (A-73)

8

$$\lambda_{HB}^{(3)} = \lambda_{TB}^{(3)} = \lambda_{LB}^{(3)} = \lambda_{AB}^{(3)} = 12.55$$
 (A-74)

9

$$\lambda_{TG}^{(i)} = 0.693$$
 (*i* = 1,2,3) (A-75)

10

$$\lambda_{AL}^{(1)} = 0.00068 \left[1 - \exp(-0.046m_A^{1.62})\right]$$
 (A-76)

11

$$\lambda_{AL}^{(i)} = \frac{1}{4} \lambda_{AB}^{(i)} \qquad (i = 2,3)$$
(A-77)

12

$$\lambda_{AT}^{(i)} = 0.012 \exp(-0.11m_A^{1.76}) +$$

$$0.00068 \exp(-0.046m_A^{1.62}) \quad (i = 1, 2, 3)$$
(A-78)

13

$$\lambda_A^{(1)} = \lambda_{AL}^{(1)} + \lambda_{AT}^{(1)} + \lambda_{AB}^{(1)} =$$
(A-79)
0.012 exp(-0.11m\_A^{1.76}) + 0.00086

14

15

$$\lambda_A^{(2)} = \lambda_{AL}^{(2)} + \lambda_{AT}^{(2)} + \lambda_{AB}^{(2)} = 0.012 \exp(-0.11m_A^{1.76}) + 0.00068 \exp(-0.046m_a^{1.62}) + 0.0161$$
(A-80)

$$\lambda_A^{(3)} = \lambda_{AL}^{(3)} + \lambda_{AT}^{(3)} + \lambda_{AB}^{(3)} = 0.012 \exp(-0.11m_A^{1.76}) + 0.00068 \exp(-0.046m_A^{1.62}) + 15.7$$
(A-81)

2

3 where  $\lambda_{XY}^{(i)}$  is the unit of day<sup>-1</sup>, and  $m_A \cong m_A^{(1)}$  is the particle burden (in mg) in the alveolar

4 compartment.

5 Experimental data on the deposition and clearance of DPM in humans are not available. To estimate the lung burden of DPM for human exposure, it is necessary to extrapolate the 6 7 transport rates  $\lambda_{xy}^{(i)}$  from rats to humans. For organics, it is assumed that the transport rates are the 8 same for rats and humans. This assumption is based upon the observation of Schanker et al. 9 (1986) that the lung clearance of inhaled lipophilic compounds appears to depend only on their 10 lipid/water partition coefficients and is independent of species. In contrast, the transport rates of diesel soot in humans should be different from those of rats, since the alveolar clearance rate,  $\lambda_A$ , 11 12 of insoluble particles at low lung burdens for human adults is approximately seven times that of 13 rats (Bailey et al., 1982).

14 No data are available on the change of the alveolar clearance rate of insoluble particles in 15 humans due to excessive lung burdens. It is seen from Equation A-79 that  $\lambda_A^{(1)}$  for rats can be 16 written in the form

17

$$\lambda_A^{(1)} = a \exp(-bm_A^c) + d \tag{A-82}$$

18

19 where a, b, c, and d are constants. The right-hand side of Equation A-82 consists of two terms, 20 representing, respectively, macrophage-mediated mechanical clearance and clearance by 21 dissolution. The first term depends upon the lung burden, whereas the second term does not. 22 To extrapolate this relationship to humans, we assume that the dissolution clearance term is 23 independent of species and that the mechanical clearance term for humans varies in the same 24 proportion as in rats under the same unit surface particulate dose. This assumption results in the 25 following expression for  $\lambda_A^{(1)}$  in humans

26

$$\lambda_A^{(1)} = \frac{a}{P} \exp[-b(m_A/S)^c] + d$$
 (A-83)

where P is a constant derived from the human/rat ratio of the alveolar clearance rate at low lung
burdens and S is the ratio of the pulmonary surface area between humans and rats. Equation
A-83 implies that rats and humans have equivalent amounts of biological response in the lung to
the same specific surface dose of inhaled DPM.

From the data of Bailey et al. (1982), a value of λ<sup>(1)</sup><sub>A</sub> = 0.00169 day<sup>-1</sup> is obtained for
humans at low lung burdens leading to P = 14.4. A value for S of 148 is reported from the data
of the anatomical lung model of Schum and Yeh (1979) for rats and Weibel's model for human
adults. For humans less than 25 years old, the model assumes the same value for P, but S is
computed from the data of the lung model for young humans (Yu and Xu 1987). The value of S
for different ages is shown in Table A-3.

12 The equations for other transport rates that have a lung-burden-dependent component are 13 extrapolated from rats to humans in a similar manner. The following lists the values of  $\lambda_{XY}^{(i)}$ 14 (in day<sup>-1</sup>) for humans used in the present model calculation:

15

$$\lambda_{HG}^{(1)} = 1.73 \ (i = 1, 2, 3) \tag{A-84}$$

16

$$\lambda_{HB}^{(1)} = \lambda_{TB}^{(1)} = \lambda_{LB}^{(1)} = \lambda_{AB}^{(1)} = 0.00018$$
 (A-85)

17

$$\lambda_{HB}^{(2)} = \lambda_{TB}^{(2)} = \lambda_{LB}^{(2)} = \lambda_{AB}^{(2)} = 0.0129$$
 (A-86)

18

$$\lambda_{HB}^{(3)} = \lambda_{TB}^{(3)} = \lambda_{LB}^{(3)} = \lambda_{AB}^{(3)} = 12.55$$
 (A-87)

19

$$\lambda_{TG}^{(i)} = 0.693$$
 (*i* = 1,2,3) (A-88)

20

$$\lambda_{AL}^{(1)} = 0.00068 \{ 1 - 0.0694 \exp[-0.046(m_A/S)^{1.62}] \}$$
(A-89)

21

$\sim$	
· )	
_	

$$\lambda_{AL}^{(i)} = \frac{1}{4} \lambda_{AB}^{(i)}$$
 (*i* = 2, 3) (A-90)

$$\lambda_{AT}^{(i)} = 0.0694 \{ 0.012 \exp[-0.11(m_A/S)^{1.76}] + (A-91) \\ 0.00068 \exp[-0.046(m_A/S)^{1.76}] \} (i = 1, 2, 3)$$

$$\lambda_A^{(1)} = \lambda_{AL}^{(1)} + \lambda_{AB}^{(1)} + \lambda_{AT}^{(1)} =$$

$$0.0694 \{ 0.012 \exp[-0.11(m_A/S)^{1.76}] \} + 0.00086$$
(A-92)

3

12 13 14

16

18 19

## 4 A.7. RESULTS

## 5 A.7.1. Simulation of Rat Experiments

6 To test the accuracy of the model, simulation results are obtained on the retention of DPM 7 in the rat lung and compared with the data of lung burden and lymph node burden obtained by 8 Strom et al. (1988). A particle size of 0.19  $\mu$ m MMAD and a standard geometric deviation,  $\sigma_g$ , of 9 2.3 (as used in Strom's experiment) are used in the calculation.

The respiratory parameters for rats are based on their weight and calculated using the
following correlations of minute volume, respiratory frequency, and growth curve data.

$$Minute volume = 0.9W (cm3/min)$$
(A-95)

15 Respiratory frequency = 
$$475W^{-0.3}$$
 (1/min) (A-96)

17 where W is the body weight (in grams) as determined from the equation

$$W = 5+537T/(100+T)$$
, for T  $\ge$  56 days (A-97)

$$\lambda_{A}^{(2)} = \lambda_{AL}^{(2)} + \lambda_{AT}^{(2)} + \lambda_{AB}^{(2)} =$$
 (A-93)

$$0.0694\{0.012 \exp[-0.11(m_A/A)^{1.76}] +$$

$$0.00068 \exp[-0.046(m_A/S)^{1.76}] + 0.016$$
(A-94)

#### 20 in which T is the age of the rat measured in days.

- 1 Equation A-95 was obtained from the data of Mauderly (1986) for rats ranging in age 2 from 3 mo to 2 years old; Equation A-96 was obtained from the data of Strom et al. (1988); and 3 Equation A-97 was determined from the best fit of the experimental deposition data. Figures A-3 and A-4 show the calculated lung burden of diesel soot  $(m_A^{(l)} + m_T^{(l)})$  and lymph node burden, 4 5 respectively, for the experiment by Strom et al. (1988) using animals exposed to DPM at 6 mg/ $m^3$ 6 for 1, 3, 6, and 12 weeks; exposure in all cases was 7 days/week and 20 h daily. The solid lines 7 represent the calculated accumulation of particles during the continuous exposure phase and the 8 dashed lines indicate calculated post-exposure retention. The agreement between the calculated 9 and the experimental data for both lung and lymph node burdens during and after the exposure 10 periods was very good.
- Comparison of the model calculation and the retention data of particle-associated BaP in 11 12 rats obtained by Sun et al. (1984) is shown in Figure A-5. The calculated retention is shown by 13 the solid line. The experiment of Sun et al. consisted of a 30-min exposure to diesel particles coated with [<sup>3</sup>H] benzo[a]pyrene ( $[^{3}H]$  - BaP) at a concentration of 4 to 6 µg/m<sup>3</sup> of air and 14 followed by a post-exposure period of over 25 days. The fast and slow phase of  $(\int_{a}^{3}H] - BaP$ 15 clearance half-times were found to be 0.03 day and 18 days, respectively. These correspond to 16  $\lambda_{AO}^2 = 0.0385 \text{ day}^{-1} \text{ and } \lambda_{AO}^{(3)} = 23.1 \text{ day}^{-1} \text{ in our model, where } \lambda_{AO}^{(i)} \text{ is the value of } \lambda_{XY}^{(i)} \text{ at } m_A \rightarrow 0.$ 17 18 Figure A-5 shows that the calculated retention is in excellent agreement with the experimental 19 data obtained by Sun et al. (1984).
- 20 21

#### A.7.2. Predicted Burdens in Humans

22 Selected results of lung burden predictions in humans are shown in Figures A-6 to A-9. The particle conditions used in the calculation are 0.2  $\mu m$  MMAD with  $\sigma_{g}$  = 2.3, and the mass 23 24 fractions of the rapidly and slowly cleared organics are each 10% ( $f_1 = f_2 = 0.1$ ). Figures A-6 25 and A-7 show, respectively, the lung burdens per unit concentration of diesel soot and the associated organics in human adults for different exposure patterns at two soot concentrations, 26 0.1 and 1 mg/m<sup>3</sup>. The exposure patterns used in the calculation are (a) 24 h/day and 7 days week; 27 28 (b) 12 h/day and 7 days/week; and (c) 8 h/day and 5 days/week, simulating environmental and 29 occupational exposure conditions. The results show that the lung burdens of both diesel soot and 30 the associated organics reached a steady-state value during exposure. Because of differences in 31 the amount of particle intake, the steady-state lung burdens per unit concentration were highest 32 for exposure pattern (a) and lowest for exposure pattern (b). Also, increasing soot concentration 33 from 0.1 to 1 mg/m<sup>3</sup> increased the lung burden per unit concentration. However, the increase was 34 not noticeable for exposure pattern (c). The dependence of lung burden on the soot concentration 35 is caused by the reduction of the alveolar clearance rate at high lung burdens discussed above.

Figures A-8 and A-9 show the effect of age on lung burden, where the lung burdens per 1 2 unit concentration per unit weight are plotted versus age. The data of lung weight at different 3 ages are those reported by Snyder (1975). The exposure pattern used in the calculation is 4 24 h/day and 7 days/week for a period of 1 year at the two soot concentrations, 0.1 and 1 mg/m<sup>3</sup>. 5 The results show that, on a unit lung weight basis, the lung burdens of both soot and organics are 6 functions of age, and the maximum lung burdens occur at approximately 5 years of age. Again, for any given age, the lung burden per unit concentration is slightly higher at  $1 \text{ mg/m}^3$  than at 7 8  $0.1 \text{ mg/m}^3$ .

9

10

## A.8. PARAMETRIC STUDY OF THE MODEL

11 The deposition and clearance model of DPM in humans, presented above, consists of a 12 large number of parameters that characterize the size and composition of diesel particles, the 13 structure and dimension of the respiratory tract, the ventilation conditions of the subject, and the 14 clearance half-times of the diesel soot and the particle-associated organics. Any single or 15 combined changes of these parameters from their normal values in the model would result in a 16 change in the predicted lung burden. A parametric study has been conducted to investigate the 17 effects of each individual parameter on calculated lung burden in human adults. The exposure 18 pattern chosen for this study is 24 h/day and 7 days/week for a period of 10 years at a constant 19 soot concentration of  $0.1 \text{ mg/m}^3$ . The following presents two important results from the 20 parametric study.

21 22

#### A.8.1. Effect of Ventilation Conditions

The changes in lung burden due to variations in tidal volume and respiratory frequency are 23 24 depicted in Figures A-10 and A-11. Increasing any one of these ventilation parameters increased 25 the lung burden, but the increase was much smaller with respect to respiratory frequency than to 26 tidal volume. This small increase in lung burden was a result of the decrease in deposition 27 efficiency as respiratory frequency increased, despite a higher total amount of DPM inhaled. 28 The mode of breathing has only a minor effect on lung burden because switching from nose 29 breathing does not produce any appreciable change in the amount of particle intake into the lung (Yu and Xu, 1987). All lung burden results presented in this report are for nose breathing. 30

31 32

#### A.8.2. Effect of Transport Rates

33 Transport rates have an obvious effect on the retention of DPM in the lung after 34 deposition. Because we are mainly concerned with the long-term clearance of diesel soot and the 35 associated organics, only the effects of two transport rates,  $\lambda_A^{(1)}$  and  $\lambda_A^{(2)}$ , are studied. Experimental

1	data of $\lambda_A^{(I)}$ from various diesel studies in rats have shown that $\lambda_A^{(I)}$ can vary by a factor of two or
2	higher. We use a multiple of 0.5 to 2 for the uncertainty in $\lambda_A^{(1)}$ and $\lambda_A^{(2)}$ to examine the effect on
3	lung burden. Figures A-12 and A-13 show respectively, the lung burden results for diesel soot
4	and the associated organics versus the multiples of $\lambda_A^{(1)}$ and $\lambda_A^{(2)}$ used in the calculation. As
5	expected, increasing the multiple of $\lambda_A^{(I)}$ reduced the lung burden of diesel soot with practically
6	no change in the organics burden (Figure A-12), while just the opposite occurred when the
7	multiple of $\lambda_A^{(2)}$ was increased (Figure A-13).
8	
9 10	A.9. OPERATIONAL DERIVATION OF HUMAN EQUIVALENT CONCENTRATIONS (HECs)
11	The model of Yu et al. (1991) is ordered into two parts; one part parameterized on the
12	physiology and anatomy of a 300 g rat and the other part parameterized on the physiology and
13	anatomy of a 25 year old human male. The sequence of steps taken to calculate the human
14	equivalent continuous concentrations (the HECs), outlined in Table A-4, were as follows:
15	
16	• The exposure scenario of the rats was entered into the rat portion of the model and the
17	model ran to obtain the output of lung burden in mg DPM/ rat lung at the time of the
18	sacrifice of the rats.
19	• The output of mg DPM/ rat lung was normalized to mg DPM/ cm <sup>2</sup> of rat lung tissue
20	based on a total pulmonary surface area of 4090 cm <sup>2</sup> .
21	• The normalized rat lung burdens were used to calculate the corresponding lung burden
22	based on the pulmonary surface area of 627,000 cm <sup>2</sup> . This operation yielded mg
23	DPM / lung of a 25 year old human male.
24	• Various air concentrations were run in an iterative fashion with the human portion of
25	the model under a continuous exposure scenario of 24 hrs/day, 7d/wk for 70 years
26	with ventilatory parameters set at 0.926 L for tidal volume and 15 breaths per minute
27	as the respiratory frequency to yield a total daily pulmonary volume of 20 m <sup>3</sup> . This
28	was continued until the output (mg DPM/lung) was matched to the mg DPM /human
29	lung obtained from the normalized rat lung burden; the concentration from the model
30	that matched this lung burden was termed the human equivalent continuous
31	concentration, the HEC. The human modeling runs did not consider the preadult
32	status of airway and alveoli number discussed above but rather were ran for 1 to
33	70 years with adult (25 years of age) parameters mentioned above.
34	

1	These HEC values address kinetic issues of DPM deposition and retention in the lung by
2	humans. As noted above, these values do not reflect the kinetic variability that may exist in the
3	human population exposed to DPM which includes men and women, young and old. However,
4	the limited parametric analysis of the model clearly shows variability of those parameters most
5	determinative in humans (e.g., tidal volume, respiration rate, and rates of clearance of particles
6	from the airways) were mirrored in the corresponding output of the model (lung burden of DPM).
7	One interpretation of this parallel in parameter-output is that the variability in the physiological
8	characteristics of humans reflects the variability in the model such that, for example, a small tidal
9	volume would be reflected with a decreased lung burden of DPM. Variability among humans of
10	these key parameters such as tidal volume do vary but within an order of magnitude. This would
11	mean that the DPM dose received by different individuals in the population from the same
12	concentration would indeed vary within the extremes of these determinative parameters.

Generation number	Number of airways	Length (cm)	Diameter (cm)	Accumulative volume <sup>a</sup> (cm)
1	1	2.680	0.340	0.243
2	2	0.715	0.290	0.338
3	3	0.400	0.263	0.403
4	5	0.176	0.203	0.431
5	8	0.208	0.163	0.466
6	14	0.117	0.134	0.486
7	23	0.114	0.123	0.520
8	38	0.130	0.112	0.569
9	65	0.099	0.095	0.615
10	109	0.091	0.087	0.674
11	184	0.096	0.078	0.758
12	309	0.073	0.070	0.845
13	521	0.075	0.058	0.948
14	877	0.060	0.049	1.047
15	1,477	0.055	0.036	1.414
16 <sup>b</sup>	2,487	0.035	0.020	1.185
17	4,974	0.029	0.017	1.254
18	9,948	0.025	0.016	1.375
19	19,896	0.022	0.015	1.595
21	39,792	0.020	0.014	2.003
22	79,584	0.019	0.014	2.607
25	318,336	0.017	0.014	7.554
24	636,672	0.017	0.014	13.784

Table A-1. Lung model for rats at total lung capacity

<sup>a</sup>Including the attached alveoli volume (number of alveoli =  $3 \times 10^7$ , alveolar diameter = 0.0086 cm). <sup>b</sup>Terminal bronchioles.

Generation number	Number of airways	Length (cm)	Diameter (cm)	Accumulative volume <sup>a</sup> (cm)
0	1	10.260	1.539	19.06
2	2	4.070	1.043	25.63
2	4	1.624	0.710	28.63
3	8	0.650	0.479	29.50
4	16	1.086	0.385	31.69
5	32	0.915	0.299	33.75
6	64	0.769	0.239	35.94
7	128	0.650	0.197	38.38
8	256	0.547	0.159	41.13
9	512	0.462	0.132	44.38
10	1,024	0.393	0.111	48.25
11	2,048	0.333	0.093	53.00
12	4,096	0.282	0.081	59.13
13	8,192	0.231	0.070	66.25
14	16,384	0.197	0.063	77.13
15	32,768	0.171	0.056	90.69
16 <sup>b</sup>	65,536	0.141	0.051	109.25
17	131,072	0.121	0.046	139.31
18	262,144	0.100	0.043	190.60
19	524,283	0.085	0.040	288.16
20	1,048,579	0.071	0.038	512.94
21	2,097,152	0.060	0.037	925.04
22	4,194,304	0.050	0.035	1,694.16
23	8,388,608	0.043	0.035	3,000.00

 Table A-2. Lung model by Weibel (1963) adjusted to 3000 cm<sup>3</sup> lung volume

Age (year)	Surface area	
0	4.99	
1	17.3	
2	27.6	
3	36.7	
4	44.7	
5	51.9	
6	58.5	
7	64.6	
8	70.4	
9	76.0	
10	81.4	
11	86.6	
12	91.6	
13	96.4	
14	101	
15	106	
16	110	
27	115	
28	119	
19	123	
20	128	
21	132	
22	136	
23	140	
24	144	
25	148	

 Table A-3. Ratio of pulmonary surface areas between humansand rats as a function of human age

Study	Exposure conditions <sup>a</sup>	Rat exposure concs (mg/m <sup>3</sup> )	mg DPM/ rat lung (modeled) <sup>b</sup>	mg DPM/cm <sup>2</sup> rat&human lung <sup>b,c</sup>	mg DPM/ human lung <sup>c</sup>	HEC (mg/m <sup>3</sup> ) <sup>c</sup>
Mauderly et al., 1987a	7 h/day, 5 days/wk, 130 wk <sup>d</sup>	0.35	0.28	6.85E-5	43	0.038
Mauderly et al., 1987a	7 h/day, 5 days/wk, 130 wk	3.47	20.23	4.95E-3	3101	1.375
Mauderly et al., 1987a	7 h/day, 5 days/wk, 130 wk	7.08	44.52	1.09E-2	6825	3.05
Ishinishi et al., 1988 (LD <sup>c</sup> )	16 h/day, 6 days/wk, 130 wk	0.11	0.24	5.87E-5	37	0.032
Ishinishi et al., 1988 (LD)	16 h/day, 6 days/wk, 130 wk	0.41	1.00	2.45E-4	153	0.128
Ishinishi et al., 1988 (LD)	16 h/day, 6 days/wk, 130 wk	1.18	18.45	4.51E-3	2828	1.25
Ishinishi et al., 1988 (LD)	16 h/day, 6 days/wk, 130 wk	2.32	39.89	9.75E-3	6115	2.75
Ishinishi et al., 1988 (HD)	16 h/day, 6 days/wk, 130 wk	0.46	1.15	2.81E-4	176	0.144
Ishinishi et al., 1988 (HD)	16 h/day, 6 days/wk, 130 wk	0.96	12.94	3.16E-3	1984	0.883
Ishinishi et al., 1988 (HD)	16 h/day, 6 days/wk, 130 wk	1.84	31.22	7.63E-3	4786	2.15
Ishinishi et al., 1988 (HD)	16 h/day, 6 days/wk, 130 wk	3.72	64.67	1.58E-2	9914	4.4
Nikula et al., 1995	16 h/day, 5 days/wk, 100 wk	2.44	28.64	7.00E-3	4391	1.95
Nikula et al., 1995	16 h/day, 5 days/wk, 100 wk	6.3	76.15	1.86E-2	11674	5.1
Heinrich et al., 1995	18 h/day, 5 days/wk, 104 wk	0.84	3.83	9.4E-4	587	0.33
Heinrich et al., 1995	18 h/day, 5 days/wk, 104 wk	2.5	34.4	8.4E-3	5274	2.35

 Table A-4. Human equivalent continuous concentrations (HECs) calculated with the model of Yu et al. (1991) from long-term repeated exposure rat studies of DPM exposure

Study	Exposure conditions <sup>a</sup>	Rat exposure concs (mg/m <sup>3</sup> )	mg DPM/ rat lung (modeled) <sup>b</sup>	mg DPM/cm <sup>2</sup> rat&human lung <sup>b,c</sup>	mg DPM/ human lung <sup>c</sup>	HEC (mg/m <sup>3</sup> ) <sup>c</sup>
Heinrich et al., 1995	18 h/day, 5 days/wk, 104 wk	6.98	97.8	2.4E-2	14993	6.7

<sup>a</sup> These are entered into the program as hrs/day, days/week for the total number of weeks exposed and the last week of exposure before evaluation (as this would affect clearance). The parameters for the rat were based on a body weight which was set in the program at 300g.

<sup>b</sup> These values were obtained with the rat portion of the model and are noted as lung burden, in mg DPM /lung of a 300 g rat, at the final week of the exposure scenario. These outputs were then normalized to cm<sup>2</sup> of the rat lung, at 4090 cm<sup>2</sup> total (Xu and Yu, 1987).

<sup>c</sup> Preparatory to using the human portion of the model, the mg DPM/cm<sup>2</sup> value from above was used to project the mg DPM that would be present in the adult human lung based on a total lung surface area of 627,000 cm<sup>2</sup> (Xu and Yu, 1987). Various air concentrations were then entered into the human model as 70 years continuous exposure scenarios and ran iteratively until the output (in mg DPM / lung at age 70) matched this mg DPM/human lung, i.e., the total lung burden. This matching air concentration is, by definition, the human equivalent continuous concentration (HEC).

<sup>d</sup> weeks = (months of exposure)  $\times$  4.33.

7/25/00

DRAFTA-3DO NOT CITE OR QUOTE

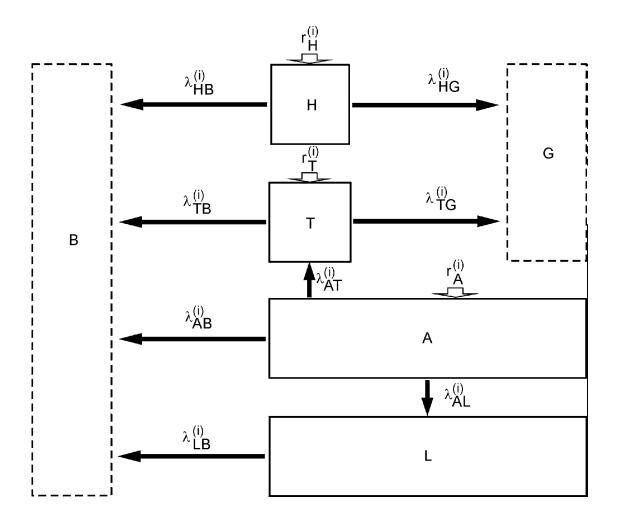


Figure A-1. Compartmental model of DPM retention.

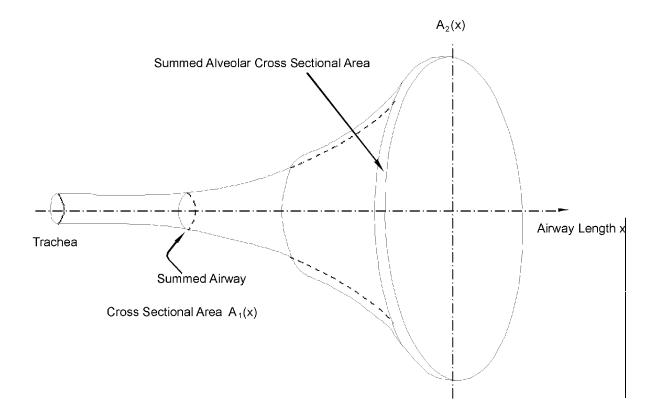


Figure A-2. Trumpet model of lung airways.

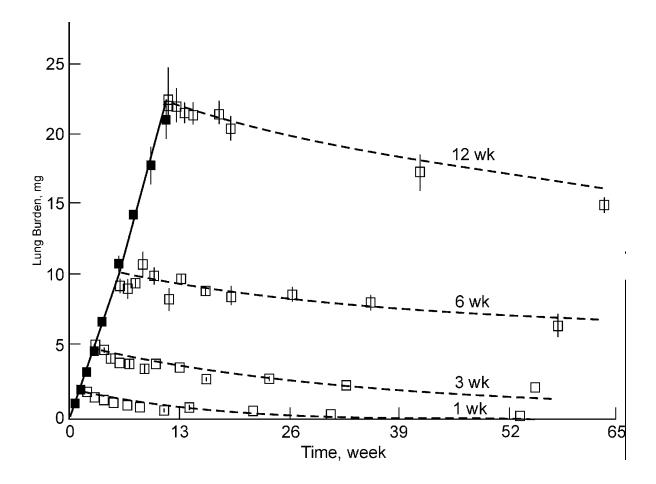


Figure A-3. The experimental and predicted lung burdens of rats to DPM at a solid and dashed concentration of 0.6 mg/m<sup>3</sup> for different exposure spans. Lines are, respectively, the predicted burdens during exposure and post-exposure. Particle characteristics and exposure pattern are explained in the text. The symbols represent the experimental data from Strom et al. (1988).

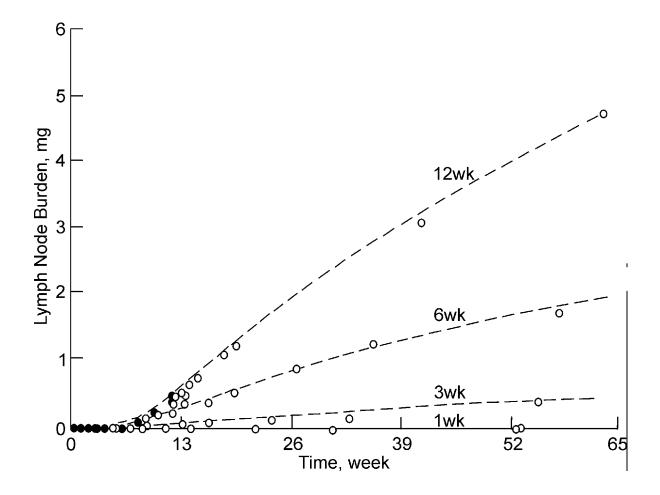


Figure A-4. Experimental and predicted lymph node burdens of rats exposed to CEPs at a concentration of 6.0 mg/m<sup>3</sup> for different exposure spans. The solid and dashed lines are, respectively, the predicted burdens during exposure and post-exposure. Particle characteristics and exposure pattern are explained in the text. The symbols represent the experimental data from Strom et al. (1988).

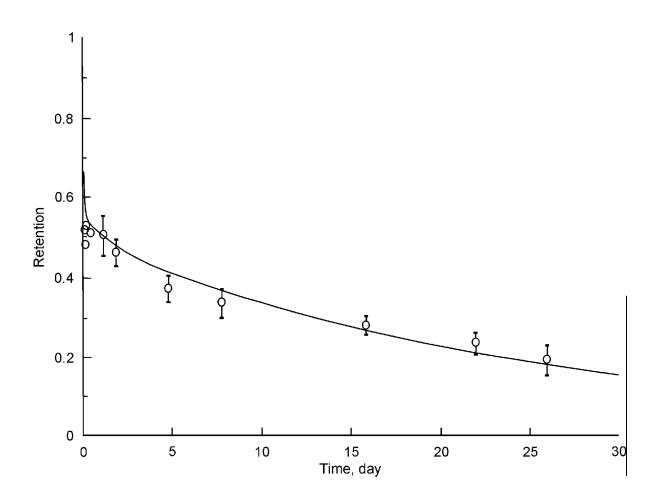


Figure A-5. Comparison between the calculated lung retention (solid line) and the experimental data obtained by Sun et al. (1984) for the particle-associated BaP in rats.

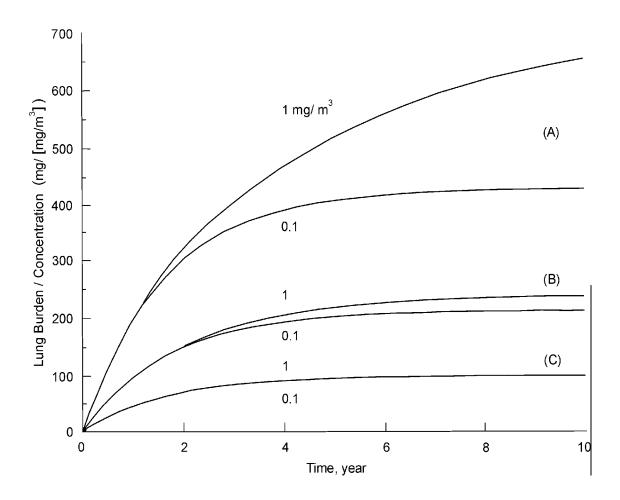


Figure A-6. Calculated lung burdens of diesel soot per unit exposure concentration in human adults exposed continuously to DPM at two different concentrations of 0.1 and 1.0 mg/m<sup>3</sup>. Exposure patterns are (a) 24 h/day and 7 days/week, (b) 12 h/day and 7 days/week, and (c) 8 h/day and 5 days/week.

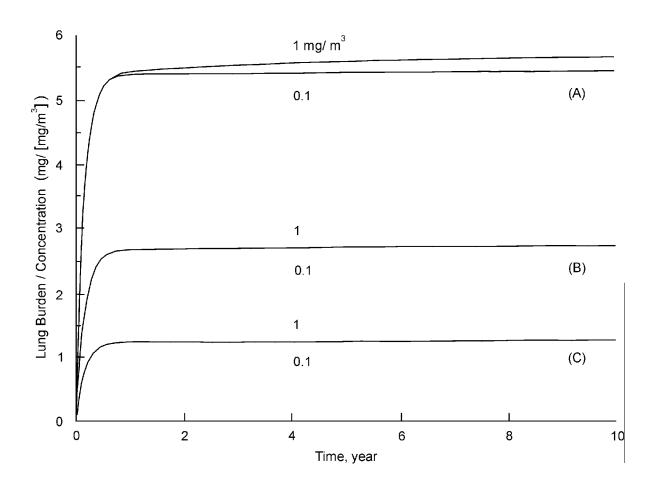


Figure A-7. Calculated lung burdens of the particle-associated organics per unit exposure concentration in human adults exposed continuously to DPM at two different concentrations of 0.1 and 1.0 mg/m<sup>3</sup>. Exposure patterns are (a) 24 h/day and 7 days/week, (b) 12 h/day and 7 days/week, and (c) 8 h/day and 5 days/week.

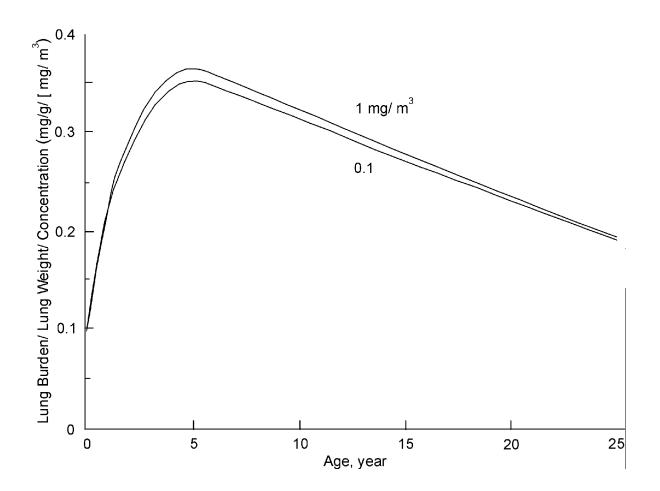


Figure A-8. Calculated lung burdens of diesel soot per gram of lung per unit exposure concentration in humans of different ages exposed continuously for 1 year to DPM of two different concentrations of 0.1 and 1.0 mg/m<sup>3</sup> for 7 days/week and 24 h daily.

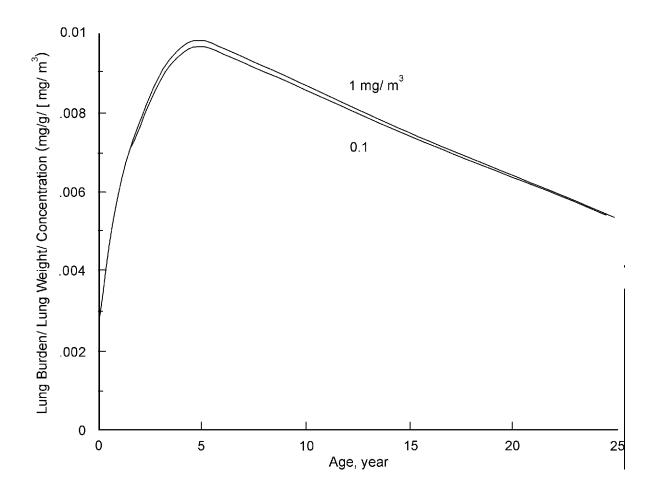


Figure A-9. Calculated burdens of the particle-associated organics per gram of lung per unit exposure concentration in humans of different ages exposed continuously for 1 year to DPM of two different concentrations of 0.1 and 1.0 mg/m<sup>3</sup> for 7 days/week and 24 h daily.

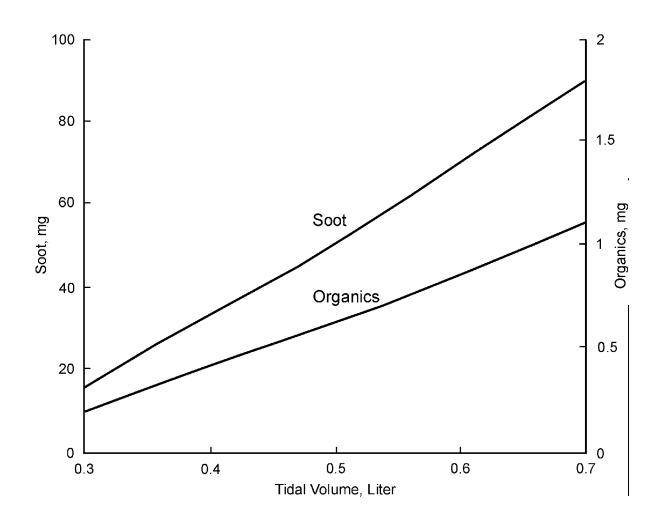


Figure A-10. Calculated lung burdens in human adults versus tidal volume in liters for exposure to DPM at 0.1 mg/m<sup>3</sup> for 10 years at 7 days/week and 24 h daily. Parameters used in the calculation are: (a) MMAD=0.2  $\mu$ m,  $\sigma_g$ =2.3,  $f_2$ =0.1,  $f_3$ =0.1; (b) respiratory frequency = 14 min<sup>-1</sup>; and (c) lung volume = 3000 cm<sup>3</sup>.

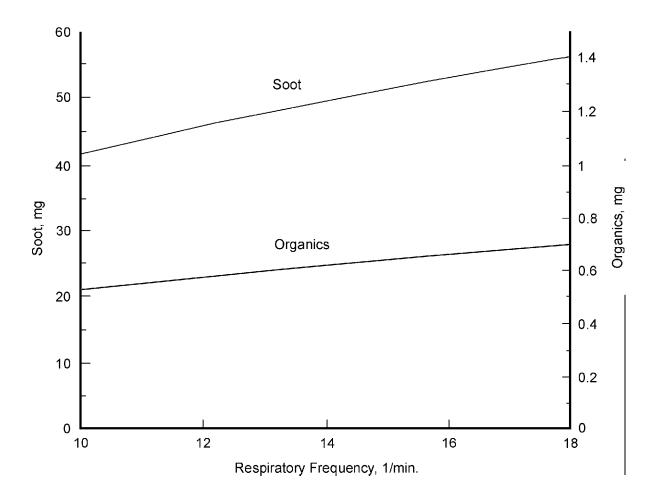


Figure A-11. Calculated lung burdens in human adults versus respiratory frequency in *bpm* for exposure to DPM at 0.1 mg/m<sup>3</sup> for 10 years at 7 days/week and 24 h daily. Parameters used in the calculation are: (a) MMAD=0.2  $\mu$ m,  $\sigma_g$ =2.3,  $f_2$ =0.1,  $f_3$ =0.1; (b) tidal volume = 500 cm<sup>3</sup>, and (c) lung volume = 3200 cm<sup>3</sup>.

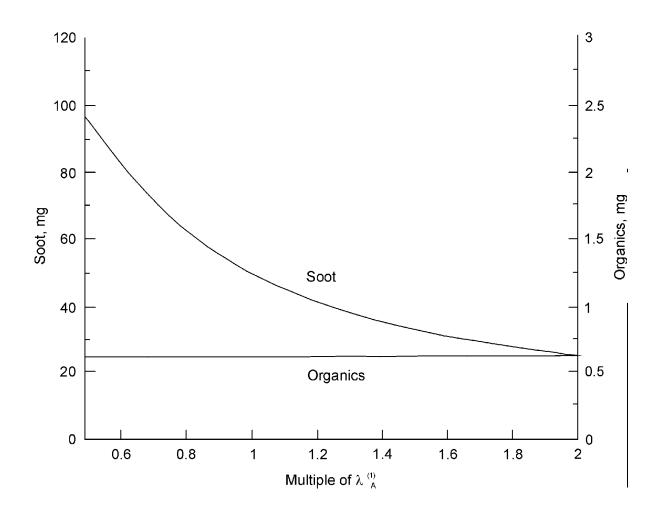


Figure A-12. Calculated lung burdens in human adults versus multiple of  $\lambda_A^{(1)}$  for exposure to DPM at 0.1 mg/m<sub>3</sub> for 10 years at 7 days/week and 24 h daily. Parameters used in the calculation are: (a) MMAD=0.2 µm,  $\sigma_g$ =2.3,  $f_2$ =0.1,  $f_3$ =0.1; (b) tidal volume = 500 cm<sup>3</sup>, respiratory frequency = 14 min<sup>-1</sup>; and (c) lung volume = 3200 cm<sup>3</sup>.

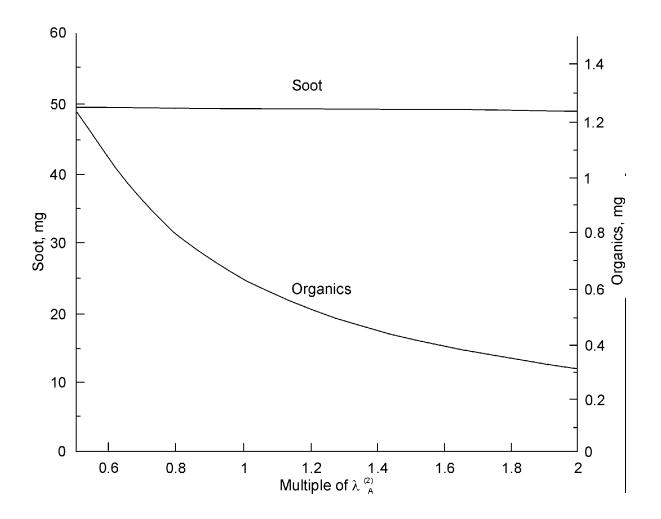


Figure A-13. Calculated lung burdens in human adults versus multiple of  $\lambda_A^{(1)}$  for exposure to DPM at 0.1 mg/m<sup>3</sup> for 10 years at 7 days/week and 24 h daily. Parameters used in the calculation are: (a) MMAD=0.2 µm  $\sigma_g$ =2.3,  $f_2$ =0.1,  $f_3$ =0.1; (b) tidal volume = 500 cm<sup>3</sup>, respiratory frequency = 14 min<sup>-1</sup>; and (c) lung volume = 3200 cm<sup>3</sup>.

# A.10. REFERENCES

1 2	Amann, CA; Siegla, DC. (1982) Diesel particles what are they and why. Aerosol Sci Technol 1:73-101.
3 4 5	Bailey, MR; Fry, FA; James, AC. (1982) The long-term clearance kinetics of insoluble particles from the human lung. Ann Occup Hyg 26:273-289.
6 7 8 9	Bond, JA; Sun, JD; Medinsky, MA; et al. (1986) Deposition, metabolism and excretion of 1-[ <sup>14</sup> C]nitropyrene and 1-[ <sup>14</sup> C]nitropyrene coated on diesel exhaust particles as influenced by exposure concentration. Toxicol Appl Pharmacol 85:102-117.
10 11 12	Chan, TL; Lee, PS; Hering, WE. (1981) Deposition and clearance of inhaled diesel exhaust particles in the respiratory tract of Fisher rats. J Appl Toxicol 1:77-82.
13 14 15	Diu, CK; Yu, CP. (1983) Respiratory tract deposition of polydisperse aerosols in humans. Am Ind Hyg Assoc J 44:62-65.
16 17	ICRP. (1979) Limits for intakes of radionuclides by workers. Ann ICRP 2. Publication 30, part 1.
18 19	Mauderly, JL. 1986. Respiration of F344 rats in nose-only inhalation exposure tubes. J Appl Toxicol 6:25-30.
20 21 22	Schanker, LS; Mitchell, EW; Brown, RA. (1986) Species comparison of drug absorption from the lung after aerosol inhalation or intratracheal injection. Drug Metab Dispos 14(1):79-88.
23 24 25	Scheutzle, D. (1983) Sampling of vehicle emissions for chemical analysis and biological testing. Environ Health Perspect 47:65-80.
26 27 28	Schum, M; Yeh, HC. (1979) Theoretical evaluation of aerosol deposition in anatomical models of mammalian lung airways. Bull Math Biol 42:1-15.
29 30	Snyder, WS. (1975) Report of task group on reference man. Oxford, London: Pergamon Press, pp. 151-173.
31 32 33 34	Solderholm, SC. (1981) Compartmental analysis of diesel particle kinetics in the respiratory system of exposed animals. Oral presentation at EPA Diesel Emissions Symposium, Raleigh, NC, October 5-7. In: Toxicological effects of emissions from diesel engines (Lewtas J, ed.). New York: Elsevier, pp. 143-159.
35 36 37 38	Strom, KA; Chan, TL; Johnson, JT. (1987) Pulmonary retention of inhaled submicron particles in rats: diesel exhaust exposures and lung retention model. Research Publication GMR-5718. Warren, MI: General Motors Research Laboratories.
39 40 41	Strom, KA; Chan, TL; Johnson, JT. (1988) Inhaled particles VI. Dodgson, J; McCallum, RI; Bailey, MR; et al., eds. London: Pergamon Press, pp. 645-658.
42 43 44	Sun, JD; Woff, RK; Kanapilly, GM; et al. (1984) Lung retention and metabolic fate of inhaled benzo(a)pyrene associated with diesel exhaust particles. Toxicol Appl Pharmacol 73:48-59.
45 46	Weibel, ER. (1963) Morphometry of the human lung. Berlin: Springer-Verlag.
47 48 49	Xu, GB; Yu, CP. (1987) Desposition of diesel exhaust particles in mammalian lungs: a comparison between rodents and man. Aerosol Sci Tech 7:117-123.
50 51	Yu, CP. (1978) Exact analysis of aerosol deposition during steady breathing. Powder Technol 21:55-62.

- Yu, CP; Diu, CK; Soong, TT. (1981) Statistical analysis of aerosol deposition in nose and mouth. Am Ind Hyg
   Assoc J 42:726-733.
   3
- Yu, CP; Xu, GB. (1986) Predictive models for deposition of diesel exhaust participates in human and rat lungs.
  Aerosol Sci Technol 5:337-347.
- 7 Yu, CP; Xu, GB. (1987) Predicted deposition of diesel particles in young humans. J Aerosol Sci 18:419-429.
- 9 Yu, CP and Yoon, KJ. (1990) Retention modeling of diesel exhaust particles in rats and humans. Res Rep Health
  10 Eff Inst 40:1-33.
- 12 Yu, CP, Yoon, KJ, and Chen, YK. (1991) Retention modeling of diesel exhaust particles in rats and humans. J.
- 13 Aerosol Med. 4(2): 79-115.

8

11